Resonance ion dissociation spectroscopy of naphthalene ions prepared in a supersonic expansion

Jack A. Syage[a] and John E. Wessel[b]
The Aerospace Corporation, P.O. Box 92957, Los Angeles, California 90009

(Received 3 March 1987; accepted 2 June 1987)

Resonance ion dissociation (RID) spectra are reported for cations of naphthalene and 2-methylnaphthalene cooled in a supersonic beam. Discrete vibronic resonances were observed in the ultraviolet region of both ions. A discrete red system was also observed for 2-methylnaphthalene that is subject to strong degenerate vibronic interaction with an underlying quasicontinuum associated with a lower energy electronic transition. This leads to effective power broadening of the RID spectra at moderately low laser intensities. The red two-photon dissociation process of 2-methylnaphthalene was successfully modeled by classical rate equations applied to a four level system, consisting of a ground state, the directly excited state, a lower energy excited state, and a final dissociative state.

I. INTRODUCTION

There is convincing evidence that multiphoton ionization fragmentation processes in aromatic hydrocarbon molecules occur by sequential mechanisms.[1] The parent ion is essentially formed instantaneously, when the neutral molecule has absorbed the minimum number of photons required to exceed the ionization threshold. Additional photons do not effectively induce transitions between continuum or autoionizing states of the neutral molecule. Subsequent photon interactions occurring in the parent ion and smaller fragments are produced by sequential absorption in successively smaller fragments, or by higher energy channels involving the parent ion. (The latter possibility is important for the ions because appearance potentials of successively smaller ion fragments are clustered in a compressed energy range.) The studies reported here seek to identify spectrally selective fragmentation processes in aromatic hydrocarbon ions via resonance ion dissociation (RID). This may prove valuable for ultrasensitive detection applications and for selective photochemistry. Our spectroscopic results for cold naphthalene and 2-methylnaphthalene cations suggest a new model for ion photofragmentation processes.

Fundamental to the understanding of laser induced ion fragmentation is knowledge about the absorption of parent and fragment ions. The spectroscopy of aromatic molecular ions has interesting properties on account of their open shell molecular orbital structure. In the simplest picture, there are absorptions in the visible region, corresponding to transitions between normally filled molecular orbitals. These are well separated from the parent molecule absorption bands in the near ultraviolet. In some instances, sequential multiphoton absorption, with vibrational redistribution between absorption of each successive red photon, should induce ion dissociation. For many species, one ultraviolet photon exceeds the dissociation threshold. Therefore, ion absorption spectra can be measured by monitoring dissociation.

Singly charged cations of numerous aromatics have been studied in a variety of low temperature matrices.[2,3] In many cases, corresponding spectra have also been recorded by ion cyclotron resonance (ICR) spectroscopy under low pressure gas phase conditions,[4–6] where ionization is induced by electron impact and spectroscopy is performed using laser or incoherent light sources. In this technique, the absorbed light induces fragmentation of the parent ion, thereby causing a loss of ICR signal. Similar results were also reported for ambient temperature samples using multiphoton ionization with laser induced ion fragmentation.[7] Freiser and Beauchamp[5] proposed a mechanism for ion fragmentation studied by ICR whereby the ion absorbs a photon in an electronic transition originating from the ground state. Internal conversion then redistributes the energy into ground state vibrational excitation. Additional photons are then successively absorbed by the same electronic transition.

Recently, Andrews and co-workers[3] reported helium temperature matrix spectra of naphthalene ions that revealed resolved vibronic structure. The linewidths were broader than those normally observed for matrix isolated neutral molecules. However, it was not known if this represented homogeneous intramolecular interactions, or inhomogeneous matrix induced broadening. This observation of discrete structure motivated our studies of the visible and ultraviolet spectroscopy of ultracold naphthalene and methylnaphthalene ions prepared in a supersonic molecular beam. The results provide new information on the spectroscopy of isolated ions and on the mechanism of multiphoton ionization fragmentation. Ionization was performed using excitation conditions that conserve the initial rotational and translational energy distributions of the cold neutral molecules, producing ions in the vibrationless level, or a single, low energy vibrational level of the parent ion [well below the threshold for intramolecular vibrational relaxation (IVR) processes in the S_1 state of the neutral molecule,[8] and presumably below the IVR threshold for the ground state of the ion]. The selectively prepared ions were dissociated by a moderately high intensity laser beam that was scanned across the ion absorption spectrum. A time-of-flight mass spectrometer was used to individually monitor both the par-

[a] Aerophysics Laboratory.
[b] Chemistry and Physics Laboratory.

 0021-9606/87/183313-08$02.10

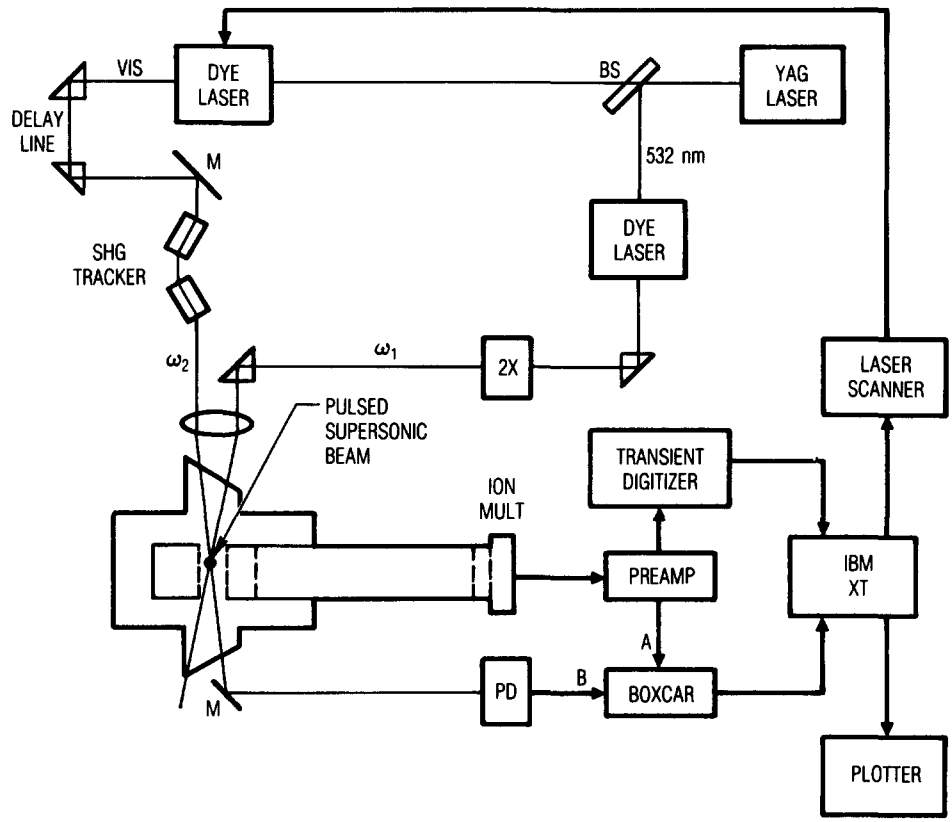

FIG. 1. Schematic of the experimental apparatus. A home-built grazing incidence dye laser is used to generate ω_1 (UV) and a commerical scanning dye laser to produce ω_2 (UV and VIS). BS = beamsplitter, M = mirror, SHG = single harmonic generation, and PD = photodiode.

ent ion and fragment ion species as a function of fragmenting wavelength. Therefore, multiphoton excitation spectra of cold ions are recorded by monitoring dips in the parent ion signal or increases in fragment ion signals. (In previous work in this[9] and other laboratories,[10] nominally similar dips in ion current were used to observe excited state transitions of neutral molecules.) The naphthalene cation must absorb four 600 nm photons in order to reach the minimum energy dissociation threshold,[6] corresponding to either loss of C_2H_2 or loss of H. The methylnaphthalenes require absorption of two 600 nm photons to reach the minimum energy dissociation threshold,[6] which corresponds to loss of one hydrogen atom.

II. EXPERIMENTAL

A supersonic molecular beam time-of-flight (TOF) mass spectrometer, depicted in Fig. 1, was constructed to study resonance ion dissociation in cold aromatic ions. The vacuum system consists of differentially pumped source and ionization chambers. A third stage of differential pumping is provided at the detector end of the TOF drift tube. A temperature controlled magnetic solenoid pulsed nozzle[11] in the source chamber was used for the supersonic expansion which enters the ionization chamber through a 1 mm skimmer. Typical expansion conditions were 50 psi He passing over naphthalene at about 75 °C. Ions were accelerated into a zero field drift region of length 1 m, where they are detected by a Johnston multiplier. Space focusing conditions were met by applying extraction and acceleration fields of 200 and 1800 V, respectively, across 1 cm grid spacing. For field sensitive experiments, the extraction field was reduced to 50 V/cm. A deflector plate system steered ions to the detector. Conventional one-color photoionization spectra confirmed that supersonic cooling was achieved. Gated TOF mass detection was used to record the RID spectra.

Excitation sources consisted of two dye lasers which were pumped by a frequency doubled Q-switched Nd:YAG laser. The ω_1 ionizing laser closely resembles the grazing incidence laser designs of Littman and Metcalf and by Shoshan, Danon, and Oppenheim.[12] This source was amplified by an external dye amplifier, frequency doubled, and aligned to overlap with the ω_2 dissociating beam (from a Quanta Ray PDL-1 dye laser). Pulse durations of both beams were about 5 ns. The amplified fundamental pulse from the grazing incidence laser was 1 mJ or less in energy, the ultraviolet beam from this laser was about 20 μJ, and the fundamental from the commercial dye laser had energies typically ranging from 1 to 10 mJ per pulse. The commercial laser beam was either used directly, or was frequency doubled (20–200 μJ/pulse) and recollimated for ultraviolet scans. The intensity of the red beam was controlled during spectral scans by changing the Nd:YAG pump intensity incident on the dye laser with a rotatable half-wave plate. Intensity was monitored with a spectrally flat photodiode or a thermopile based detector. Ultraviolet scans reported in this paper were performed without active control of laser intensity. The ionizing and dissociating beams were focused into the ionization region of the molecular beam by a 30 cm focal length lens. A spherical lens was used for high intensity investigations, and a cylindrical lens was used for routine measurements, where minimum power broadening was desired.

III. RESULTS

Experiments are reported on 2-methylnaphthalene and naphthalene. Some measurements were performed on 1-methylnaphthalene, but the results do not contribute to the findings. The methylnaphthalene ions dissociate at lower total energy; therefore they were better candidates for spectroscopic study in the red region, where two-photon dissociation is possible. Both naphthalene and 2-methylnaphthalene RID spectra were studied in the near ultraviolet region. One-photon absorption exceeds the dissociation threshold for the methylnaphthalene ions, presumably inducing rapid predissociation, whereas two-photon absorption is required to dissociate naphthalene ions.

Naphthalene ions were produced in single vibronic levels by resonance two-photon ionization by ω_1. The $b_{3g}(8)$ level (henceforth, $^+\bar{8}$ where the + sign refers to the cation) was populated by the excitation process $(\bar{8}^1 8^1 \leftarrow 0_0) + (^+\bar{8}_1 \leftarrow \bar{8}^1 8^1)$ at $\omega_1 = 301.61$ nm. A small contribution ($\sim 10\%$) of vibrationless ions, $^+0_0$, is formed based on prior measurements.[13] Pure excitation of the $^+0_0$ level of naphthalene ion was achieved by $(7^1 \leftarrow 0_0) + (^+0_0 \leftarrow 7^1)$ excitation at $\omega_1 = 302.96$ nm. For 2-methylnaphthalene, lack of adequate knowledge of Franck–Condon factors and mode assignments make vibrational excitation in the ion difficult to assess. Two-photon threshold ionization studies[14] and reported S_1 excitation wavelengths[15] of the methylnaphthalenes indicate that the $^+0_0$ level of 2-methylnaphthalene ions is exclusively produced by $2\omega_1$ excitation at 310.8 nm. At 308.3 nm, $^+\bar{8}_1$ ion formation is energetically favored, although some admixture of $^+0_0$ is expected to occur.

The red induced ion dissociation spectrum of the 2-methylnaphthalene ion is presented in Fig. 2. Spectra were pieced together from scans over several dye gain curves. Excitation pulse energy was maintained moderately constant over the regions scanned. Both parent ion (M^+) loss and fragment ion ($[M-1]^+$ for loss of one hydrogen) formation displayed essentially the same spectral dependence, as shown in the figure. (The ratio of $[M-1]^+$ to M^+ signal intensity was maintained less than or equal to 0.3 in the red dissociation region.) The spectra display vibronic structure closely resembling that observed previously[3] in the low temperature rare gas matricies, with a red shift of 200 cm^{-1} for the origin in the matrix. Vibrational features were observed at 422 ± 15 cm^{-1} and 830 ± 15 cm^{-1} above the origin, as compared to intervals of 444 cm^{-1} and 875 cm^{-1} reported by Andrews *et al.*[3] The red induced dissociation spectra in the supersonic molecular beam show a continuum of considerable amplitude (about 50% of the maximum dip amplitude) that extends to the red of the origin, at least as far as 810 nm. The continuum fragmentation signals were also apparent in spectra recorded using the $[M-1]^+$ mass, as shown in Fig. 2(b). Continuum absorption was not clearly evident in the prior low temperature matrix spectra, presumably because it is difficult to judge 100% transmission in these measurements. The vibronic transition linewidths were highly sensitive to intensity, and approached 200 cm^{-1} at the lowest intensities employed, which is considerably larger than the 160 cm^{-1} reported for an argon matrix. At

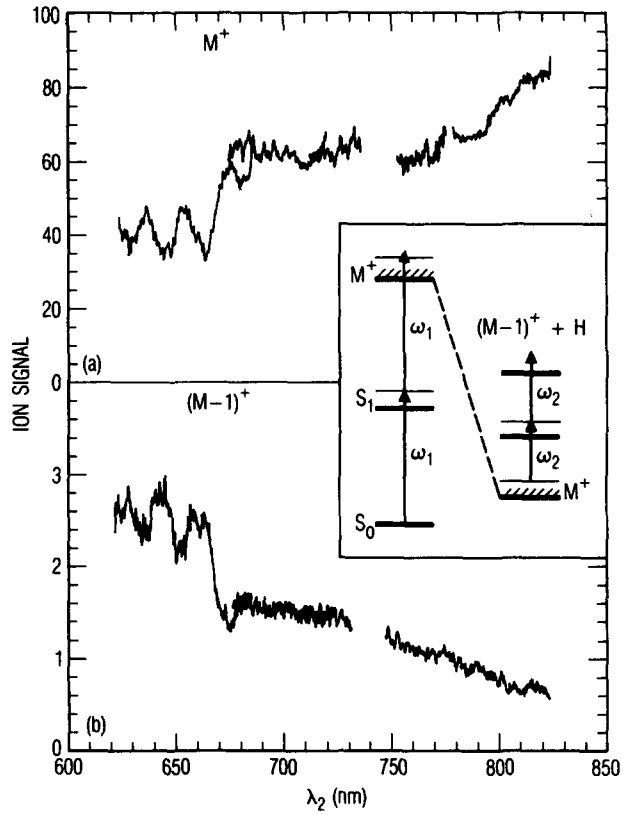

FIG. 2. Resonance ion dissociation (RID) spectra of 2-methylnaphthalene (2-MeN) cation via low energy electronic states. (a) M^+ molecular ion dip spectrum, and (b) $[M-1]^+$ fragment ion formation spectrum. R2PI excitation by ω_1 at 308.3 nm populates the $^+\bar{8}_1$ state of the molecular cation (insert): Delayed excitation by ω_2 reveals a diffuse ion absorption at very low energy and a structured absorption at higher energy. The ω_2 ion dip intensity in (a) is relative to full scale (which represents the ion signal in the absence of ω_2). The unit of intensity in (b) is arbitrary. The spectra were pieced together from 1 mJ constant energy scans involving several laser dyes.

the red ω_2 intensities normally used to optimize fragmentation, the spectra broadened to the extent that they resembled those of uncooled ions. Parent M^+ loss and fragment $[M-1]^+$ formation spectra, recorded at two different intensities, are presented in Fig. 3. Dissociation was approximately linearly dependent on intensity for excitation in the 2-methylnaphthalene ion continuum region, as shown in Fig.4.

Extensive studies were carried out in the near ultraviolet region, in search of evidence for dissociation induced by discrete one-photon absorption by the ion. We also found evidence of autoionizing Rydberg features above the ionization threshold, which will be discussed in a following publication. For these mesurements, the ω_1 and the ω_2 lasers were each capable, independently, of inducing strong ionization. Therefore, these one-laser signals were identified and overlooked in the search for ion signals that depend on the action of both $\omega_1 + \omega_2$. In the case of interest, the ω_2 laser scans over the various ionization thresholds (such as the lowest ion zeropoint threshold, the $^+\bar{8}$ threshold at about + 450 cm^{-1}, and the $^+7$ threshold at about + 1000 cm^{-1}), generating a continuum ionization signal. When ω_2 becomes resonant with an ion transition in the ultraviolet, parent ion dis-

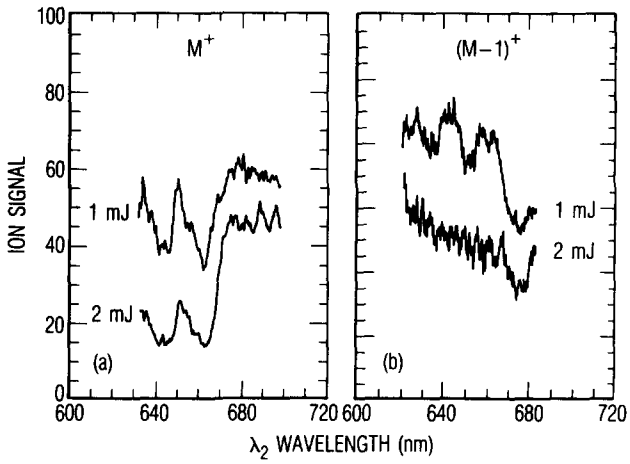

FIG. 3. Dependence on ω_2 pulse energy for the vibrationaly-resolved RID spectra of 2-MeN cation formed by R2PI at 308.3 nm (a) M^+ ion dip spectra where full scale is the ion signal in the absence of ω_2. (b) $[M-1]^+$ ion formation spectra. The unit of intensity in (b) is arbitrary, however the intensity of the spectra relative to each other is accurate.

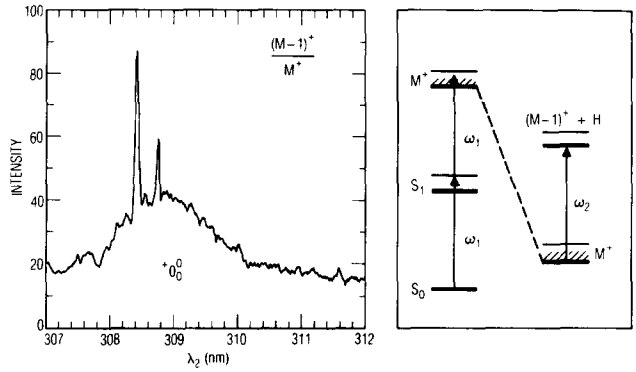

FIG. 5. RID spectrum of 2-MeN cation via ω_2 UV excitation. R2PI excitation by ω_1 at 310.8 nm populates the vibrationless level of the cation (i.e., $^+0_0$). Delayed excitation by ω_2 reveals the rather broad $^+0_0^0$ cation transition. The RID process involving H atom loss is conveniently monitored via the ratio of ion signals, $[M-1]^+/M^+$. The sharp features occur by accidental ω_2 R2PI of neutral 2-MeN followed by ω_2 RID of the cation to give $[M-1]^+$. If a resonance absorption by M^+ to form $[M-1]^+$ *did not* occur by the ω_2 only route, then the sharp features would be negative going in the ratio spectrum.

sociation increases, causing a dip in the otherwise spectrally continuous parent ion signal. This dip is expected to be slightly to the blue of 307.6 nm for the naphthalene cation, and to the blue of 312.0 nm for 2-methylnaphthalene cations, based on low temperature argon matrix results.

We observed a prominent transition, centered at $\omega_2 = 308.8$ nm, for the 2-methylnaphthalene ion, as shown in Fig. 5, where the signal is displayed as the ratio $[M-1]^+/M^+$ in order to enhance sensitivity. Higher energy vibronic transitions were not observed, presumably due to the limited signal-to-noise ratio. The corresponding transition for naphthalene, shown in Fig. 6, was observed in spectral regions where ionization thresholds occur by $\omega_1 + \omega_2$ excitation (where ω_2 is scanned). Naphthalene ion dissociation was recorded in terms of depletion of the parent ion signal, relative to the continuum ion signals generated by the sum of one color signals for ω_1 plus ω_2. If there were no ion dissociation, the spectrum would consist of only threshold steps. For Fig. 6(a), this corresponds to ω_2 crossing the threshold for $|^+0\rangle \leftarrow |S_1\rangle$ (i.e., IP_0). For Fig. 6(b), this corresponds to ω_2 exceeding the threshold for excitation of $^+\bar{8}_1$ in the ion (i.e., IP_0). The decrease in parent ion signal centered at about 304.7 nm in Fig. 6(a) and 6(b), is a consequence of parent ion dissociation induced by ω_2. As a check,

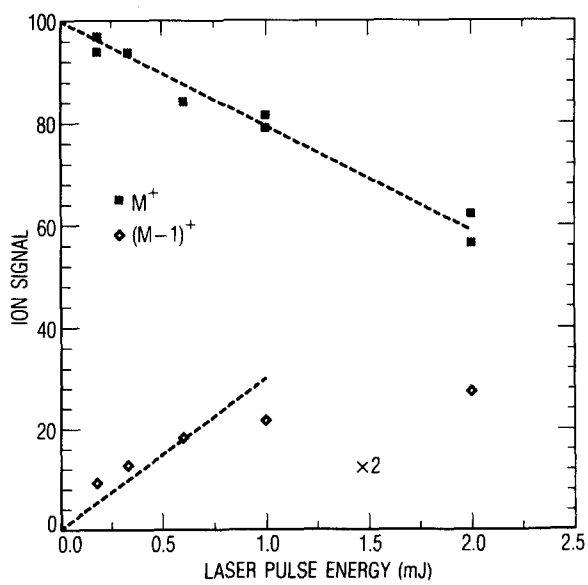

FIG. 4. Dependence on ω_2 pulse energy for the M^+ and $[M-1]^+$ RID ion signals via excitation of the low energy diffuse state of the 2-MeN cation. ($\lambda_1 = 308.3$ nm and $\lambda_2 = 765$ nm.) The relative intensity scale for M^+ and $[M-1]^+$ is approximate. The dashed line is provided for convenience.

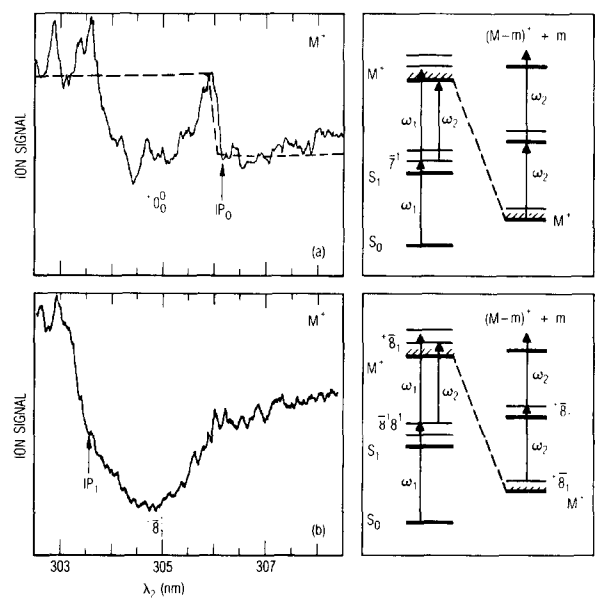

FIG. 6. RID spectra for different vibronic states of naphthalene cation. Ion dip spectra for M^+, along with the corresonding excitation scheme, are given for; (a) vibrationless $^+0_0$ cations formed by ω_1 R2PI excitation at 302.96 nm, and (b) $^+\bar{8}_1$ cations formed by ω_1 excitation at 301.61 nm. Ion formation by $\omega_1 + \omega_2$ is identifiable by ionization threshold. These are denoted by $IP_0 = \omega_1(7^1 \leftarrow 0_0) + \omega_2(^+0_0 \leftarrow 7^1)$ and $IP_1 = \omega_1(\bar{8}^1 8^2 \leftarrow 0_0) + \omega_2(^+\bar{8}_1 \leftarrow \bar{8}^1 8^1)$. The ion threshold response due to $\omega_1 + \omega_2$ only, without fragmentation, is approximated for IP_0 by the dotted line in (a). The extraction field in the ionization region was 50 V/cm.

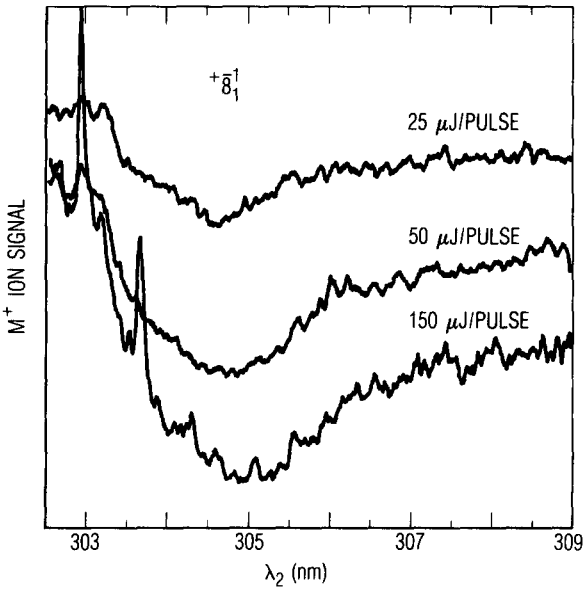

FIG. 7. Dependence on ω_2 pulse energy for the $^+\bar{8}_1^1$ RID ion dip spectrum of naphthalene cation formed by ω_1 R2PI at 301.61 nm. Spectra are arbitrarily offset on the vertical scale.

a spectrum was recorded for total ion count (thereby summing M^+ and $[M\text{-}m]^+$), in which case the dip disappeared. The decrease of M^+ was highly dependent on ω_2 pulse energy. The 304.5 nm dip was not observed at low intensity, whereas at high intensity, the step at 306 nm essentially vanished in the broadened 304.5 nm dip. For the argon matrix, the ion transition occurs at 307.6 nm, corresponding to a red shift of 300 cm^{-1}. In the gas phase the linewidth is approximately 90 cm^{-1}, measured at the lowest intensities, which is close (possibly within experimental error) to the 60 cm^{-1} linewidth reported for the argon matrix. The intensity dependence of the ion absorption feature (with ions prepared in the $^+\bar{8}$ state) is shown in Fig. 7. There is evidence of power broadening and possibly a spectral shift, which may be induced by intensification of the neighboring 303.5 nm ionization transition of the neutral molecule.

RID spectra for fragment ion formation resulting from UV excitation of naphthalene cation are given in Fig. 8. The spectra, plotted as the ratio of fragment to parent ion signal, compare the 0_0^0 and $^+\bar{8}_1^1$ transition for H atom loss. Direct detection of C_2H_2 loss is also illustrated for the $^+\bar{8}_1^1$ transition. All of these spectra are similar, within experimental uncertainty.

IV. DISCUSSION

Cold ion dissociation spectra, measured at moderate intensities, were spectrally continuous, essentially identical to ambient temperature spectra observed previously by ICR and MPI techniques. Discrete spectral structure was expected for the cooled ions, based on the two-photon model for the dissociation process, which was initially proposed for the methylnaphthalenes by Dunbar and co-workers,[6] and previously, for other molecules by Freiser and Beauchamp.[5] In this model, the first photon excites the ion to an electronic state that rapidly relaxes, by intramolecular vibrational re-

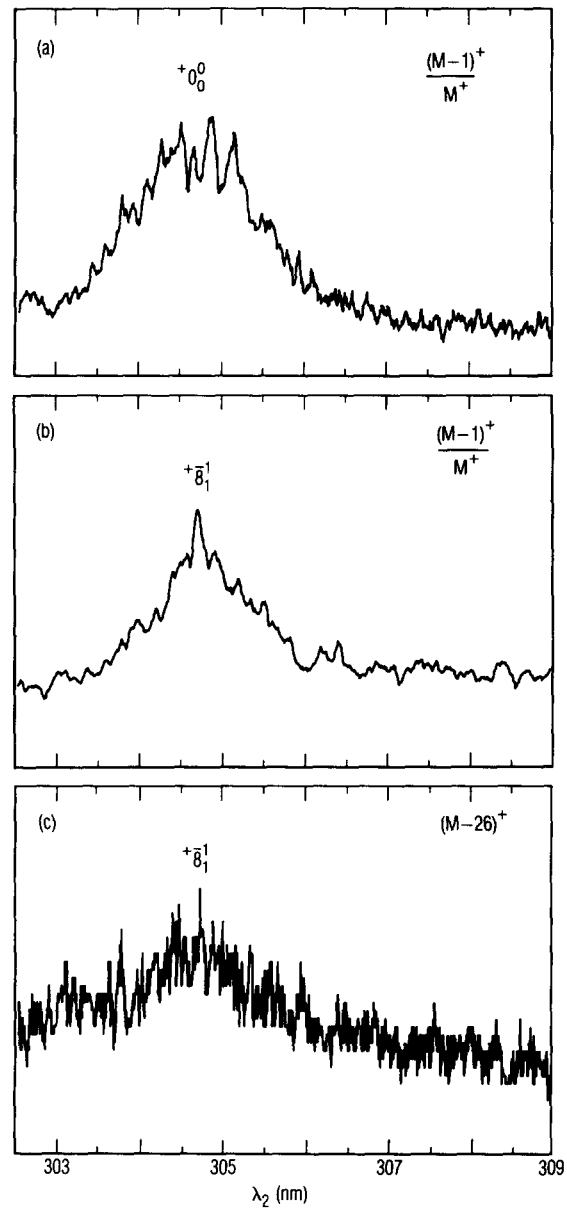

FIG. 8. RID fragment ion formation spectra from state-selected naphthalene cation. The H atom loss channel is monitored by the ratio $[M-1]^+/M^+$. The C_2H_2 dissociative channel is perceptible via direct detection of $[M-26]^+$ using the same resonance excitation process as in (b). Excitation conditions are given in Fig. 6.

distribution, to vibrational excitation in the ground state. The ground electronic state then absorbs a second red photon, via the same ground state electronic transition, and thereby exceeds the dissociation threshold energy. The lack of spectral structure in our spectra suggested a power broadening mechanism, in which red transitions of the cool ions are saturated, even relatively far from resonance. However, the peak intensities typically employed in these experiments were about 10^8 W/cm^2. We estimate an effective peak red one-photon absorption cross section for cooled 2-methylnaphthalene to be $\leqslant 10^{-16}$ cm^2, based on Dunbar's measured peak red cross section at ambient temperature, of about 10^{-17} cm^2. This implies a power broadened width of $\leqslant 2$ cm^{-1} for the red system, assuming power broadening is approximately equal to the Rabi frequency for the transition.

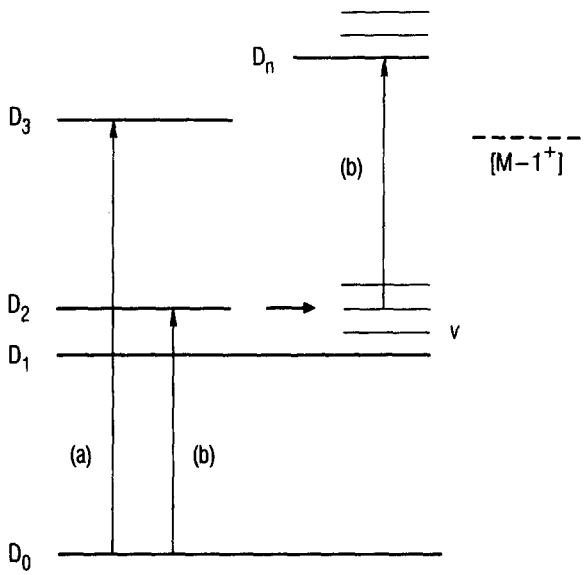

FIG. 9. Energy level diagram for the methylnaphthalene ion with the proposed model for ultraviolet induced one-photon and red induced two-photon dissociation processes. One-photon ultraviolet induced dissociation, via the excited doublet state D_n, is shown in (a). Two-photon red induced dissociation, via the dipole allowed $D_2 \leftarrow D_0$ transition, is depicted in (b). This excitation is accompanied by an IVR process that leads to non-Franck–Condon active vibrational population in the D_1 Therefore, the $D_n \leftarrow D_1$ transition is weak, requiring high intensity to produce $[M-1]^+$ fragment ions efficiently.

This is much narrower than that observed in our beam measurements.

A key to resolving this discrepancy is the observation of strong continuum background fragmentation signal to wavelengths longer than the red transition origin. This was observed for all the naphthalene species studied and at all experimentally accessible intensities. Furthermore, the mass spectra, induced with the red beam tuned to the low energy continuum, were essentially identical to those observed in direct resonance with discrete red transitions. Apparently, the prior low temperature matrix studies were not sensitive to this continuum absorption.

We propose that the background contribution to the fragmentation spectrum is due to a quasicontinuous absorption system associated with a lower energy electronic transition of the ion. The lower transition will be denoted $D_1 \leftarrow D_0$, where D_0 represents the ground doublet state of the ion, and D_1 represents the first excited doublet state of the ion. $D_1 \leftarrow D_0$ corresponds to a formally forbidden transition of the naphthalene cation, between the highest energy completely filled orbital and the half-filled highest energy orbital. This one-photon transition will be vibronically active in the region of the red transition, which is denoted $D_2 \leftarrow D_0$ in Fig. 9, the energy level diagram describing the model. There will be a high density of vibronically active modes of D_1 in the vicinity of D_2, which is about 4000 cm^{-1} above the expected D_1 origin. By analogy with neutral naphthalene and other aromatic species which display strong resonant vibronic interaction between the S_2 and S_1 states,[16] we expect a near continuum of vibronic background absorption in the region of D_2. Thus, the real source of broadening will be degenerate vibronic interaction between D_2 and D_1, rather than simple power broadening of a Lorentzian $D_2 \leftarrow D_0$ transition. The first photon effectively excites highly excited D_1 vibrational levels. If this state has a substantial lifetime, the second photon will induce a $D_n \leftarrow D_1$ transition that may have a spectrum drastically altered, relative to $D_2 \leftarrow D_0$. Thus, much higher intensities may be required to drive this second absorption step efficiently within the short duration of the ω_2 laser pulse. At the high fluence required, effective saturation will occur for both the $D_2 \leftarrow D_0$ absorption peaks and the background continuum transition.

The saturation process can be modeled qualitatively by a simple rate equation treatment. We assume that excitation via $D_2 \leftarrow D_0$ results in the immediate production of vibrationally excited D_1 states, at a rate, $R_{2\leftarrow 0}$, given by the product of the cross section, $\sigma_{2\leftarrow 0}$ and the ω_2 intensity. The corresponding rate for the second transition is denoted $R_{n\leftarrow 1}$, and the populations are denoted N_0 for the ground state, N_1 for the D_1 state, and N_n for the dissociated ion, where it is assumed that the parent ion state, D_n, dissociates rapidly, relative to the excitation process. Given these assumptions, the incoherent rate equations are:

$$\dot{N}_0 = -R_{2\leftarrow 0} \times N_0, \tag{1}$$

$$\dot{N}_1 = R_{2\leftarrow 0} \times N_0 - \frac{N_1}{T}, \tag{2}$$

$$\dot{N}_n = R_{n\leftarrow 1} \times N_1. \tag{3}$$

In the case of interest, we assume that T is large relative to the other terms in Eq. (2), and we assume that the effective T_2 for the level excited by the first photon is extremely short, as is expected for IVR processes in naphthalene excited with over 4000 cm^{-1} excess vibrational energy. The laser pulse duration was taken to be 5 ns and $\sigma_{n\leftarrow 1}$, the cross section for the second transition, was assumed to be spectrally independent, with a value of 1×10^{-18} cm^2.

The population N_n, calculated as a function of the cross section $\sigma_{2\leftarrow 0}$, is shown in Fig. 10, for various ω_2 intensities.

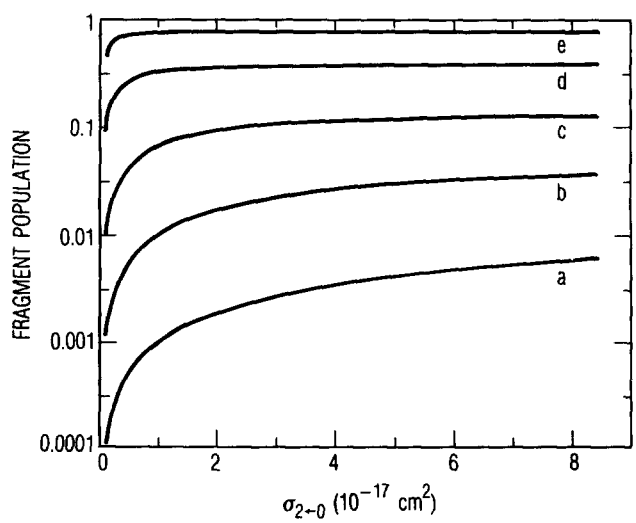

FIG. 10. Calculated population of the final ion fragment as a function of cross section for the (2←0) transition. Results are plotted for several experimental intensities, using the experimental laser pulse duration of 5 ns (a) 1×10^6 W/cm^2, (b) 3×10^6 W/cm^2, (c) 1×10^7 W/cm^2, (d) 3×10^7 W/cm^2, and 1×10^8 W/cm^2.

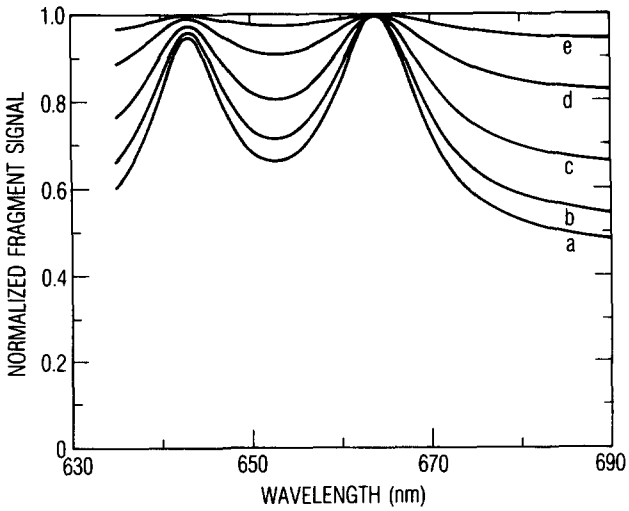

FIG. 11. Power broadening of a simulated methylnaphthalene $D_2 \leftarrow D_0$ spectrum with continuum background calculated as a function of ω_2 intensity: (a) 0 W/cm^2, (b) 1×10^6 W/cm^2, (c) 3×10^6 W/cm^2, (d) 10^7 W/cm^2, and (e) 3×10^7 W/cm^2. The fragment ion signals (population of $|n\rangle$) are normalized at 662 nm in order to facilitate comparison of line shapes.

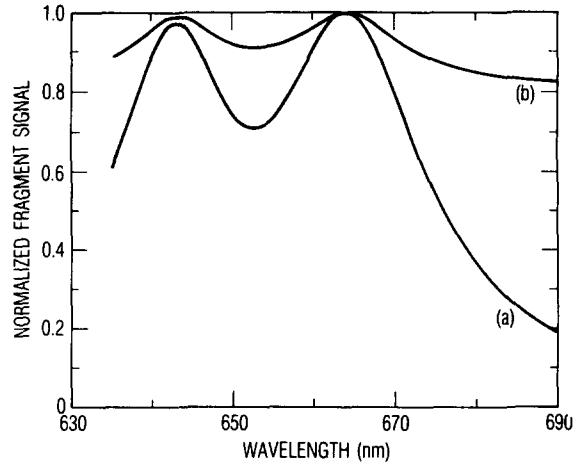

FIG. 12. Power broadening at 10^7 W/cm^2 of 2-methylnaphthalene ion dissociation calculated for (a) simulated $D_2 \leftarrow D_0$ spectrum without continuum background, and (b) simulated $D_2 \leftarrow D_0$ spectrum with continuum background. The fragment ion signals (population of $|n\rangle$) are normalized at 662 nm in order to facilitate comparison of line shapes.

(Our typical experiments employ approximately 10^7 W/cm^2 effective intensity in TEM_{00} at ω_2. In the discussion we refer to intensities, whereas fluence is a more appropriate variable for the model. Analytical expressions for similar situations are given by Koplitz and McVey[17].) Clearly, the N_n population, and thus, the fragmentation signal, are effectively saturated under moderate intensity excitation conditions. In this case, the slope of the population N_n vs $\sigma_{2\leftarrow0}$, is nearly zero. Reducing intensity to the range of 10^7 W/cm^2 for the assumed 5 ns pulse duration, reduces saturation markedly for the expected range of cross sections. The above model was then used to calculate the spectral effect of power broadening for the intensities used in our experiments. Figure 11 was calculated based on an artificial low power spectrum, consisting of two Lorentzian lines, centered at the ion transition wavelengths, and superimposed on a continuum background of amplitude equal to the peak contribution of the Lorentzian 0_0^0 component. The intrinsic linewidths were assumed to be equal to the approximate measured low power linewidths of 270 cm^{-1} for the 0_0^0 transition and 230 cm^{-1} for the 400 cm^{-1} transition. (A linewidth of 160 cm^{-1} was reported for 2-methylnaphthalene in the argon matrix at 20 K.) The calculation predicts the qualitative observations of decreased modulation amplitude and increased spectral width at high intensity. In addition, it correctly predicted significantly greater dissociation at 652 nm, between spectral peaks, than for the long wavelength continuum baseline, beyond 680 nm. When smaller values were assumed for the intrinsic linewidth, calculations predicted the dissociation amplitude at 652 nm should be close to that observed at 690 nm, regardless of intensity. In Fig. 12, the power broadened spectrum is calculated based on an intrinsic (low power) spectrum, free of background absorption [Fig. 12(a)] and the result is compared to the spectrum calculated with a continuum background contribution, where both cases are subject to an intensity of 1×10^7 W/cm^2. Under our experimental conditions, noise features would largely obscure spectral structure in Fig. 12(b), whereas structure would be easily resolved in the background free case of Fig. 12(a). This strongly supports the continuum background absorption model.

In prior work with the naphthalene ions, there is no evidence of radiatively stable D_2 states. This is consistent with the proposed model, which would predict vibronically induced emission from the D_1 state, rather than D_2. No search has been made, to our knowledge, for emission from D_1 states, which would occur in the 1.4 μm region. Partial support for the model is provided by the large linewidths observed for the $D_2 \leftarrow D_0$ systems, in both molecular beam and matrix isolation studies.

This model also suggests that similar resonant vibronic interactions should occur for the ultraviolet transition system, here denoted $D_3 \leftarrow D_0$. This one-photon transition is energetically capable of inducing dissociation into the $[M-1]^+ + H$ species for 2-methylnaphthalene. This may account for the substantial linewidth observed for this transitions. Power broadening is expected to be less important for the ultraviolet system of 2-methylnaphthalene than for the red transitions, because dissociation is a one-photon process, thereby avoiding the need for high intensity to drive the second absorption step. Evidently, power broadening is not a major problem for naphthalene ions in the ultraviolet either, because the measured linewidths were about the same as observed for the substituted species. Therefore, we conclude that the two-photon process is relatively efficient in the naphthalene ion, probably due to a substantial cross section for absorption of the second photon. Nonetheless, there is evidence of power broadening for both ion species in the ultraviolet. This is attributed to the background continuum oscillator strength present in the region of the ultraviolet transitions, combined with the requirement for intensities sufficient to dissociate a substantial fraction of the ions by the laser pulse. Our limited attempts to observe higher energy $D_3 \leftarrow D_0$ vibronic transitions were unsuccessful. However,

these transitions are expected to be weak and overlapped by one-laser transitions. Therefore, it is not surprising that they were not resolved.

V. CONCLUSION

This study provides a framework for future studies of aromatic species by resonance ion dissociation techniques. Clearly, direct confirmation of the model will require more complete spectroscopy of the D_1 state. Ideally, D_1 lifetime measurements and $D_n \leftarrow D_1$ excited state absorption measurements will confirm the suggested kinetic model. Near infrared ionization–dissociation experiments will directly characterize the D_1 state. Presumably D_1 will be moderately stable, thereby permitting high resolution $D_1 \leftarrow D_0$ spectroscopy. Low energy, vibronically induced, $D_1 \leftarrow D_0$ transition should provide the ideal basis for future selective ionization–dissociation detection methods.

ACKNOWLEDGMENTS

The authors gratefully acknowledge the valuable assistance of Mr. Larry Pruitt in conducting these experiments. We also thank Mr. Eric Fournier for assistance with software development. This work was supported by the Office of Health and Environment, Department of Energy under Contract No. DE-FG03-ER6039.

[1]U. Boesl, H. J. Neusser, and E. W. Schlag, J. Chem. Phys. **72**, 4327 (1980); W. Dietz, H. J. Neusser, U. Boesl, E. W. Schlag, and S. H. Lin, Chem. Phys. **66**, 105 (1982); J. T. Meek, R. K. Jones, and J. P. Reilly, J. Chem. Phys. **73**, 3503 (1980); J. C. Miller and R. N. Compton, *ibid.* **75**, 22 (1981); K. R. Newton, D. A. Lichten, and R. B. Bernstein, J. Phys. Chem. **85**, 15 (1981); R. S. Pandolfi, D. A. Gobeli, and M. A. El-Sayed, *ibid.* **85**, 1779 (1982); P. Hering, A. G. M. Maaswinkel, and K. L. Kompa, Chem. Phys. Lett. **83**, 222 (1981), and references therein.

[2]G. T. Hoijtink and P. J. Zandstra, Mol. Phys. **3**, 371 (1960); T. Shida and S. Iwata, J. Am. Chem. Soc. **95**, 3477 (1973).

[3]L. Andrews, B. Kelsall, and T. A. Blankenship, J. Phys. Chem. **86**, 2916 (1982); L. Andrews, R. S. Friedman, and B. J. Kelsall, *ibid.* **89**, 4016, 4550 (1985).

[4]B. S. Freiser and J. L. Beauchamp, J. Am. Chem. Soc. **96**, 6260 (1974).

[5]B. S. Freiser and J. L. Beauchamp, Chem. Phys. Lett. **35**, 35 (1975).

[6]J. P. Honovich, J. Segell, and R. C. Dunbar, J. Phys. Chem. **89**, 3617 (1985); M. S. Kim and R. C. Dunbar, J. Chem. Phys. **72**, 4405 (1980); R. C. Dunbar and R. Klein, J. Am. Chem. Soc. **98**, 7994 (1976).

[7]D. Mordaunt, G. Loper, and J. Wessel, J. Phys. Chem. **88**, 5197 (1984).

[8]S. M. Beck, D. L. Monts, M. G. Liverman, and R. E. Smalley, J. Chem. Phys. **70**, 1062 (1979); A. Amirav, U. Even, and J. Jortner, Opt. Commun. **32**, 266 (1980); R. A. Coveleskie, D. A. Dolson, and C. S. Parmenter, J. Chem. Phys. **72**, 5774 (1980).

[9]J. A. Syage and J. E. Wessel, J. Chem. Phys. **85**, 6806 (1986); D. E. Cooper, C. M. Klimcak, and J. E. Wessel, Phys. Rev. Lett. **46**, 324 (1981); D. E. Cooper and J. E. Wessel, J. Chem. Phys. **76**, 2155 (1982).

[10]J. Murakami, K. Kaya, and M. Ito, Chem. Phys. Lett. **91**, 401 (1982); T. Suzuki, N. Mikami, and M. Ito, *ibid.* **120**, 333 (1985); M. Fujii, T. Ebata, N. Mikami, and M. Ito, J. Phys. Chem. **88**, 4265 (1984).

[11]J. A. Syage, P. M. Felker, and A. H. Zewail, J. Chem. Phys. **81**, 2233 (1984); B. W. Keelan, J. A. Syage, J. F. Shepanski, and A. H. Zewail, *International Conference Proceedings of Laser 83* (STS, McLean, VA., 1984), p. 718.

[12]M. G. Littman and H. J. Metcalf, Appl. Opt. **17**, 2224 (1978); M. G. Littman, Opt. Lett. **3**, 138 (1978); I. Shoshan, N. N. Danon, and P. Oppenheim, J. Appl. Phys. **48**, 4495 (1977).

[13]R. P. Frueholz, D. E. Cooper, C. M. Klimcak, and J. E. Wessel, J. Phys. Chem. **86**, 4892 (1982).

[14]J. A. Syage and J. E. Wessel (unpublished work).

[15]J. A. Warren, J. M. Hayes, and G. J. Small, J. Chem. Phys. **80**, 1786 (1984).

[16]J. Wessel, Ph.D. dissertation, University of Chicago, Chicago, IL, 1970; J. Wessel and D. S. McClure, Mol. Cryst. Liq. Cryst. **58**, 121 (1980).

[17]B. D. Koplitz and J. K. McVey, J. Chem. Phys. **81**, 4964 (1984); **80**, 2271 (1984).